Intrinsic UDE Control of Mechanical Systems on SO(3)

A. L. M. Sanka Liyanage, Jordan M. Berg, Beibei Ren, and D. H. S. Maithripala

***Abstract*— The uncertainty and disturbance estimation (UDE) structure provides flexible and intuitive controller design for command following and disturbance rejection in uncertain linear and nonlinear systems. In this paper, an intrinsic UDE controller is demonstrated for fully-actuated mechanical systems on SO(3), the group of rigid-body rotations in three-dimensional Euclidean space. The controller is derived in a geometric framework, thereby avoiding issues arising from any particular set of coordinates. Simulations and experiments using a quadrotor test bed show that the controller can stabilize a desired equilibrium attitude in the presence of disturbances and parameter error.**

I. Introduction

The uncertainty and disturbance estimator (UDE) control structure provides a useful control design framework for linear and nonlinear systems [1], [2], [3], [4]. The UDE approach reduces the servomechanism problem to that of selecting an appropriate filter to capture the dynamic characteristics of the commands to be tracked or the disturbances to be rejected [3]. Recent work has extended the UDE framework to time-delay systems [5], [6]. This paper considers the coordinate-free extension of the UDE framework to fully-actuated mechanical systems on Lie groups.

Geometric control design addresses the control of dynamic systems evolving on manifolds that cannot be identified with Euclidean spaces [9], [10], [11], [12]. Inherent in the manifold description is the requirement for multiple coordinate charts to describe the configuration and velocity of the system. This requirement for multiple coordinate systems naturally raises the question of which is the best choice for control design. The geometric approach to control is based on the premise that the controller itself should be described in a coordinate free, or *intrinsic*, setting [8]. Intrinsic controllers may be directly expressed in any choice of coordinates without the need for additional analysis, and with no special logic needed to handle transitions from one chart to another. Results on geometric control for tracking and disturbance rejection in SO(3) includes [9], [13], [14], [15], [16].

Deriving a coordinate-free, intrinsic UDE formulation presents several challenging obstacles. The main UDE design parameter is a filter that incorporates the dynamic properties of the commands and disturbances. The meaning of this filter is a general geometric setting, is unclear. Here we proceed from the premise that the filter should capture the physical nature of the command and disturbance signals. Hence, disturbances that are expected to be constant or slowly varying in a particular reference frame are filtered in that frame. To develop this notion more fully it is useful to focus on a particular case. Therefore this paper is concerned specifically with rigid-body attitude control, which is naturally expressed in the Lie group SO(3), the space of all rigid rotations in three spatial dimensions.

This paper is organized as follows: Section II presents the dynamic equations of a fully-actuated mechanical system on SO(3). Section III derives the UDE controller for this system. Section IV describes simulation results for attitude stabilization of a quadrotor model subject to disturbance forces and parametric uncertainty. Section V describes preliminary experimental results on a small quadrotor UAV. Finally Section VI presents our conclusions.

II. Intrinsic Governing Equations on SO(3)

The orientation of a rigid body in three-dimensional Euclidean space is an element of the Lie group $SO(3)$. The state space is the tangent bundle for $SO(3)$. We represent the attitude of the body at time t by $R(t) \in SO(3)$, where R is a 3×3 orthogonal matrix with determinant $+1$. Every $R \in SO(3)$ satisfies $R^TR = I$. Thus $\dot{R}^TR = -R^T\dot{R} = -\left(\dot{R}^TR\right)^T$, and so $\dot{R}^TR$ is an element of Skew_3, the space of 3×3 skew-symmetric matrices. The skew-symmetric matrix $R^T\dot{R}$ is the *velocity vector*. Skew_3 may be identified with $\mathbb{R}^3$ using the "hat" map,

$$\hat{\Omega} \triangleq \begin{bmatrix} 0 & -\Omega_3 & \Omega_2 \\ \Omega_3 & 0 & -\Omega_1 \\ -\Omega_2 & \Omega_1 & 0 \end{bmatrix}, \tag{1}$$

where $\Omega = [\Omega_1, \Omega_2, \Omega_3]^T \in \mathbb{R}^3$. Subsequently we refer to both $\hat{\Omega} = \dot{R}^TR$ and the corresponding Ω as the velocity vector, where the meaning should be clear from context. For further details we refer to [17], [18].

The intrinsic equations describing the evolution of $R \in SO(3)$ are [18],

$$\dot{R} = R\hat{\Omega} \tag{2}$$

$$\nabla_{\Omega}\Omega = T_u + d \tag{3}$$

where T_u is the generalized control force vector, $T_u = \mathbb{I}^{-1}\tau_u$ where τ_u is the physical control torque and $\mathbb{I}$ is the inertia matrix. Vector d is the generalized external disturbance force vector, including the generalized force equivalents arising

A. L. M. S. Liyanage is with the Department of Mechanical Engineering, Texas Tech University, Lubbock, TX 79409. sanka.liyanage@ttu.edu

J. M. Berg is with the Department of Mechanical Engineering Texas Tech University, Lubbock, TX 79409. jordan.berg@ttu.edu

B. Ren is with the Department of Mechanical Engineering Texas Tech University, Lubbock, TX 79409. beibei.ren@ttu.edu

D. H. S. Maithripala is with Department of Mechanical Engineering, University of Peradeniya, Peradeniya KY-20400, Sri Lanka. smaithri@pdn.ac.lk

from unmodeled dynamics in the body frame. $\nabla_\Omega \Omega$ is the intrinsic acceleration of the system, found as the covariant derivative of Ω along itself. The covariant derivative generalizes the notion of the directional derivative, and may be thought of as the component of the velocity vector that is tangent to the configuration manifold. For further details we refer to [11], [18]. For two velocity vectors, $\hat{\eta}, \hat{\zeta} \in \mathbb{R}_3$, at the same configuration R,

$$\nabla_\zeta \eta = \dot{\eta} + \tfrac{1}{2}\left(\zeta \times \eta - \mathbb{I}^{-1}(\mathbb{I}\eta \times \zeta + \mathbb{I}\zeta \times \eta)\right). \tag{4}$$

where $\dot{\eta}$ is the normal time derivative of η measured in the body frame [13], [14], [17]. Thus

$$\nabla_\Omega \Omega = \dot{\Omega} - \mathbb{I}^{-1}(\mathbb{I}\Omega \times \Omega). \tag{5}$$

The control objective is for the system (2)–(3) to asymptotically track a *reference system*, specified as

$$\dot{R_d} = R_d \hat{\Omega}_d \tag{6}$$
$$\nabla_{\Omega_d} \Omega_d = f_d(t) \tag{7}$$

where $f_d(t)$ is a given reference control input. We require that f_d be bounded for all t. The various results and definitions given above for (2)–(3) naturally apply to (6)–(7) as well.

III. Intrinsic UDE Control on SO(3)

A. UDE Overview

Given a system with state $x \in \mathbb{R}^n$, state equation $\dot{x} = f(x) + u + \Delta(t,x)$, where u is a control input and Δ includes both disturbance forces and modeling errors, and reference system $\dot{x}_d = f_d(x_d) + u_d(t)$, consider the problem of driving a scalar error function $\mathscr{E}(x, x_d)$ to zero. Differentiation gives

$$\dot{\mathscr{E}} = \left(\frac{\partial \mathscr{E}}{\partial x}\right)(f(x) + u + \Delta) + \left(\frac{\partial \mathscr{E}}{\partial x_d}\right)(f_d(x_d) + u_d(t))$$

to which we wish to assign the dynamics

$$\dot{\mathscr{E}} = -k\mathscr{E}.$$

Thus,

$$\left(\frac{\partial \mathscr{E}}{\partial x}\right)(f(x) + u + \Delta) = -F_d(t, x_d),$$

where $F_d(t, x_d) \triangleq k\mathscr{E} + \left(\frac{\partial \mathscr{E}}{\partial x_d}\right)(f_d(x_d) + u_d(t))$, or

$$u(x, u_d, \Delta) = -f(x) - \Delta - \left(\frac{\partial \mathscr{E}}{\partial x}\right)^{-1} F_d(t, x_d). \tag{8}$$

Note that $x_d(t)$ can be found from $u_d(t)$, the specified reference dynamics, and the initial condition $x_d(0)$. However because Δ is unknown, we cannot directly implement (8). Hence it is necessary to find an estimate $\hat{\Delta}$. In the UDE framework, this estimate is obtained based on the identity $\Delta = \dot{x} - f(x) - u$. To do this, the signal $\dot{x} - f(x) - u$ is passed through a linear filter with impulse response $g_f(t)$ to obtain

$$\hat{\Delta}(t) = g_f(t) \star \dot{x} - g_f(t) \star f(x(t)) - g_f(t) \star u, \tag{9}$$

where "$\star$" denotes convolution. To avoid the need to measure $\dot{x}$, the filter is designed to include an integrator. Substituting (9) into (8) yields the following implicit expression for u:

$$\left(\delta(t) - g_f(t)\right) \star u(t) = -(\delta(t) - g_f(t)) \star f(x(t)) - g_f(t) \star \dot{x} - \left(\frac{\partial \mathscr{E}}{\partial x}\right)^{-1} F_d(t, x_d), \tag{10}$$

where $\delta(t)$ is the delta function.

A common scenario in the UDE literature is to consider a second-order system with vector error $[x_E, v_E]^T$, where $x_E \triangleq x - x_d$ is a scalar and $v_E \triangleq \dot{x}_E$. A scalar error is defined as $\mathscr{E} = k_1 x + v$, with scalar $k_1 > 0$. Subsequently we will translate this formulation into the geometric setting for a Lie group. In that case such a scalar error will be defined for *each independently actuated degree of freedom*. The result will be separate UDE controllers for each degree of freedom, coupled by the system dynamics.

B. UDE for Fully-Actuated Systems on SO(3)

The goal of this section is to stabilize a rigid body at a desired operating attitude R_d on SO(3). Let the configuration error be $E = R_d^T R$ [17], [13], [14], [12], [15]. Then the error dynamics can be written intrinsically as,

$$\dot{E} = E\hat{\Omega}_E \tag{11}$$
$$\nabla_{\Omega_E} \Omega_E = T_u + d \tag{12}$$

where T_u is the generalized control force and d is the generalized disturbance force. $\hat{\Omega}_E = E^T \dot{E}$ is a skew symmetric matrix which consists of the error body angular velocities. It can be shown that error velocities are $\Omega_E = \Omega - E^T \Omega_d$. Next consider a polar Morse function $f : SO(3) \rightarrow \mathscr{R}$, with a unique global identity $I_{3\times 3}$. Polar Morse functions exist on any compact manifold [17]. Let $f(t) = f(E(t))$ and let the gradient be $\eta = E(t)^T \text{grad}(f(E(t)))$. Subsequently we consider the globally defined polar Morse function $f(E) = \text{tr}(I_{3\times 3} - E)$ [17]. It follows that $\widehat{I\eta} = (E - E^T)$ and $\hat{\eta} = \frac{1}{det(I)} I(E - E^T)I$. It also follows that $f(E)$ has four critical points at $E_0 = I_{3\times 3}$, $E_1 = \text{diag}\{1, -1, -1\}$, $E_2 = \text{diag}\{-1, 1, -1\}$and $E_3 = \text{diag}\{-1, -1, 1\}$, where E_0 is a global minimum and the others are local maxima [17].

Define the variable

$$\hat{\eta} = \frac{1}{det(I)} I(E - E^T)I$$
$$e = \begin{bmatrix} \eta \\ \Omega_E \end{bmatrix}_{6\times 1} \tag{13}$$

where η and Ω_E are vectors in R_3, associated with $\hat{\eta}$ and $\hat{\Omega}$ respectively.

Define the the scalar error function on SO(3)

$$\mathscr{E}_{3\times 1} = \left[(K_1)_{3\times 3} \quad I_{3\times 3}\right] e_{6\times 1} \tag{14}$$

where $K_1 = \begin{bmatrix} k_1 & 0 & 0 \\ 0 & k_1 & 0 \\ 0 & 0 & k_1 \end{bmatrix}$, where $k_1 > 0$ is a scalar. Also $\hat{\mathscr{E}}$ lies on tangent space $so(3)$, where $\hat{\mathscr{E}} = k_1\hat{\eta} + \hat{\Omega}_E$. Then,

$$\mathscr{E} = k_1 \eta + \Omega_E \quad \in \mathbb{R}_3 \tag{15}$$

Covariant derivative of the filtered tracking error

$$\nabla_{\mathscr{E}}\mathscr{E} = \nabla_{(k_1\eta+\Omega_E)}(k_1\eta+\Omega_E) \tag{16}$$

By expanding the right hand side

$$\begin{aligned}\nabla_{\mathscr{E}}\mathscr{E} &= k_1\nabla_{(k_1\eta+\Omega_E)}\eta + \nabla_{(k_1\eta+\Omega_E)}\Omega_E \\ &= k_1^2\nabla_\eta\eta + k_1\nabla_{\Omega_E}\eta + k_1\nabla_\eta\Omega_E + \nabla_{\Omega_E}\Omega_E \end{aligned} \tag{17}$$

Covariant derivative of η according to (4)

$$\nabla_\eta\eta = \dot{\eta} - \mathbb{I}^{-1}(\mathbb{I}\eta\times\eta)$$

Then (17) becomes

$$\begin{aligned}\nabla_{\mathscr{E}}\mathscr{E} &= k_1^2(\dot{\eta} - \mathbb{I}^{-1}(\mathbb{I}\eta\times\eta)) + \nabla_\Omega\Omega - E^T\nabla_{\Omega_d}\Omega_d \\ &\quad + k_1\nabla_{\Omega_E}\eta + k_1\nabla_\eta\Omega_E \end{aligned} \tag{18}$$

Substitute (3) and (7) to (18)

$$\begin{aligned}\nabla_{\mathscr{E}}\mathscr{E} &= k_1^2(\dot{\eta} - \mathbb{I}^{-1}(\mathbb{I}\eta\times\eta)) + T_u + d - E^T f_d \\ &\quad + k_1\nabla_{\Omega_E}\eta + k_1\nabla_\eta\Omega_E \end{aligned} \tag{19}$$

Following (4), the covariant derivative of $\mathscr{E}$ is

$$\nabla_{\mathscr{E}}\mathscr{E} = \dot{\mathscr{E}} - \mathbb{I}^{-1}(\mathbb{I}\mathscr{E}\times\mathscr{E}).$$

Expanding the left hand side gives

$$\begin{aligned}\dot{\mathscr{E}} - \mathbb{I}^{-1}(\mathbb{I}\mathscr{E}\times\mathscr{E}) &= k_1^2(\dot{\eta} - \mathbb{I}^{-1}(\mathbb{I}\eta\times\eta)) + T_u + d \\ &\quad - E^T f_d + k_1\nabla_{\Omega_E}\eta + k_1\nabla_\eta\Omega_E \end{aligned}$$

Thus,

$$\begin{aligned}\dot{\mathscr{E}} &= k_1^2(\dot{\eta} - \mathbb{I}^{-1}(\mathbb{I}\eta\times\eta)) + T_u + d - E^T f_d \\ &\quad + k_1\nabla_{\Omega_E}\eta + k_1\nabla_\eta\Omega_E + \mathbb{I}^{-1}(\mathbb{I}\mathscr{E}\times\mathscr{E}) \end{aligned} \tag{20}$$

Lets define $\mathscr{D} = k_1\nabla_{\Omega_E}\eta + k_1\nabla_\eta\Omega_E + d$. Then (20) becomes

$$\dot{\mathscr{E}} = k_1^2\dot{\eta} + T_u - E^T f_d + \mathbb{I}^{-1}(\mathbb{I}\mathscr{E}\times\mathscr{E}) - k_1^2\mathbb{I}^{-1}(\mathbb{I}\eta\times\eta) + \mathscr{D} \tag{21}$$

Consider

$$T_u = v + u_d \tag{22}$$

where v and u_d are stabilization term and disturbance cancellation controllers. v can be considered as

$$\begin{aligned} v &= -k_p\eta - k_d\Omega_E - k_1^2\dot{\eta} + E^T f_d - \mathbb{I}^{-1}(\mathbb{I}\mathscr{E}\times\mathscr{E}) \\ &\quad + k_1^2\mathbb{I}^{-1}(\mathbb{I}\eta\times\eta) \end{aligned} \tag{23}$$

where k_p and k_d are constants. u_d can be selected as

$$u_d = -\mathscr{D} \tag{24}$$

By subtituting (23) and (24) to (21) gives

$$\begin{aligned}\dot{\mathscr{E}} &= -k_p\eta - k_d\Omega_E \\ \dot{\mathscr{E}} &= -k\mathscr{E} \end{aligned} \tag{25}$$

where $k = k_d$ and $k_p = k_1k_d$. By substituting (22) and (23) to (21) gives

$$\dot{\mathscr{E}} = -k_p\eta - k_d\Omega_E + \mathscr{D} + u_d$$

Solving it for $\mathscr{D}$

$$\mathscr{D} = \dot{\mathscr{E}} + k_p\eta + k_d\Omega_E - u_d \tag{26}$$

Assume that $G_f(s)$ is a strictly proper low-pass filter with a unity gain. Then $\mathscr{D}$ can be approximated by [1]

$$\hat{\mathscr{D}} = g_f(t)\star(\dot{\mathscr{E}} + k_p\eta + k_d\Omega_E - u_d) \tag{27}$$

Here $\star$ is the convolution operater and $g_f(t) = \mathscr{L}^{-1}\{G_f(s)\}$ where$\mathscr{L}^{-1}\{.\}$ is the Laplace inverse operator. Selecting $u_d = -\hat{\mathscr{D}}$ substituting it to (27)

$$u_d = -g_f(t)\star(\dot{\mathscr{E}} + k_p\eta + k_d\Omega_E - u_d) \tag{28}$$

Solving (28)results in

$$u_d = -\mathscr{L}^{-1}\frac{G_f}{1-G_f}\star(\dot{\mathscr{E}} + k_p\eta + k_d\Omega_E) \tag{29}$$

Substituting (29) and (23) in to (22) gives

$$\begin{aligned} T_u &= -k_p\eta - k_d\Omega_E - k_1^2\dot{\eta} + E^T f_d - \mathbb{I}^{-1}(\mathbb{I}\mathscr{E}\times\mathscr{E}) \\ &\quad + k_1^2\mathbb{I}^{-1}(\mathbb{I}\eta\times\eta) - \mathscr{L}^{-1}\frac{G_f}{1-G_f}\star(\dot{\mathscr{E}} + k_p\eta + k_d\Omega_E) \end{aligned}$$

Assume that external disturbance bounded within the expectrum $[0, w_f]$ where $w_f > 0$ Then G_f can be taken as a first order law pass filter [7]

$$G_f = \frac{1}{1+\tau s} \tag{30}$$

where $\tau = \frac{1}{w_f} > 0$ is a time constant

$$\frac{G_f}{1-G_f} = \frac{1}{\tau s} \tag{31}$$

Equation (30) can be further simplified to

$$\begin{aligned} T_u &= -k_p\eta - k_d\Omega_E - k_1^2\dot{\eta} + E^T f_d - \mathbb{I}^{-1}(\mathbb{I}\mathscr{E}\times\mathscr{E}) \\ &\quad + k_1^2\mathbb{I}^{-1}(\mathbb{I}\eta\times\eta) - \frac{1}{\tau}(\mathscr{E} + \int_0^t (k_p\eta + k_d\Omega_E)dt) \end{aligned}$$

with (15) above equation can be further simplified to

$$\begin{aligned} T_u &= -(k_p + \frac{k_1}{\tau})\eta - (k_d + \frac{1}{\tau})\Omega_E - k_1^2\dot{\eta} - \mathbb{I}^{-1}(\mathbb{I}\mathscr{E}\times\mathscr{E}) \\ &\quad + k_1^2\mathbb{I}^{-1}(\mathbb{I}\eta\times\eta) - \frac{1}{\tau}T_I^u - E^T f_d \end{aligned} \tag{32}$$

where

$$\begin{aligned} T_I^u &= \frac{1}{\tau}\int_0^t (k_p\eta + k_d\Omega_E)dt \\ \eta &= (E - E^T) \\ \Omega_E &= (\Omega - E^T\Omega_d) \\ \dot{E} &= E\hat{\Omega}_E \end{aligned}$$

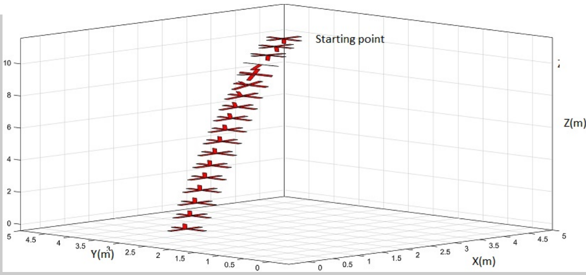

Fig. 1. Stabilization at angles $(0,0,0)$ under parametric uncertainty with initial upside-down configuration.

T_I^u can be considered as the covariant integral of $(k_p\eta + k_d\Omega_E)$.Then the following equation holds [16]:

$$\nabla_{\Omega_E} T_I^u \quad = \quad \frac{1}{\tau}(k_p\eta + k_d\Omega_E) \tag{33}$$

where

$$T_I^u \quad \triangleq \quad \begin{bmatrix} \Omega_{I1} \\ \Omega_{I2} \\ \Omega_{I3} \end{bmatrix}$$

By (4) $\nabla_{\Omega_E} T_I^u$ can be calculated as

$$\nabla_{\Omega_E} T_I^u = \dot{\Omega}_I + \frac{1}{2}(\Omega_E \times \Omega_I - \mathbb{I}^{-1}(\mathbb{I}\Omega_I \times \Omega_E + \mathbb{I}\Omega_E \times \Omega_I)) \tag{34}$$

Equation (32) with (33) forms the geometric UDE controller.

IV. Quadrotor UAV Simulation Results

We use the nominal inertial properties $M = 1.2$, I =dig$\{.005, .005, .008\}$ to calculate the thrust forces and moment T_u. We select the control parameters in (32) to be $k_p = 65, k_d = 30, k_1 = 10, \tau = .05$ and also assume that the inertia is perturbed by error ΔI =dig$\{.1, .2, .4\}$. Equations were simulated in the MATLAB environment using the ode45 function. Quaternions were used to represent the system configuration. Results, shown in Fig. 2, indicate that $\mathscr{E}$ exponentially approaches zero. Fig. 1, show the quadrotor stabilizes from initial upside configuration to hovering position

V. Quadrotor UAV Experiment Results

The UDE algorithm (32) with (33) was implemented on an AscTec Hummingbird quadrotor UAV (Ascending Technologies). The Hummingbird platform shown in the Fig. 3 includes the following equipment:

1) ZigBee RF transceiver for data acquisition and remote control.
2) Low level processor (ARM 7) for sensor and actuator interfacing.
3) High level processor (ARM 7) for system-level control.
4) IMU and GPS modules for navigation and control.

To filter out noise in the angular velocity data from the IMU, we used the following first-order discrete low-pass filter:

$$y(t_k) = \frac{T}{T+h} y(t_{k-1}) + \frac{h}{T+h} u(t_k), \tag{35}$$

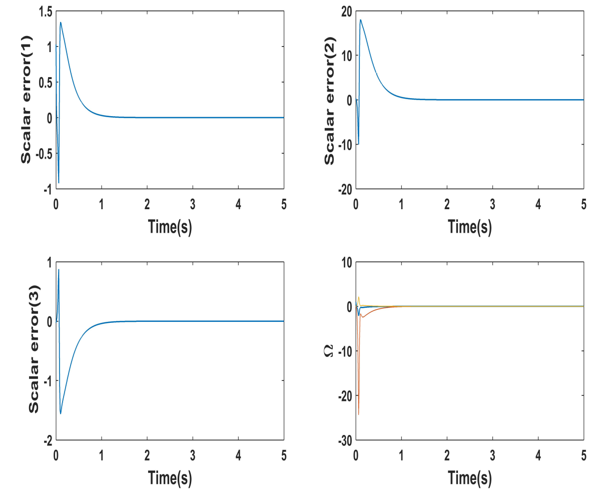

Fig. 2. Scalar error $\mathscr{E}$ and body angular velocities Ω for stabilization at angles $(0,0,0)$ under parametric uncertainty with initial upside-down configuration.

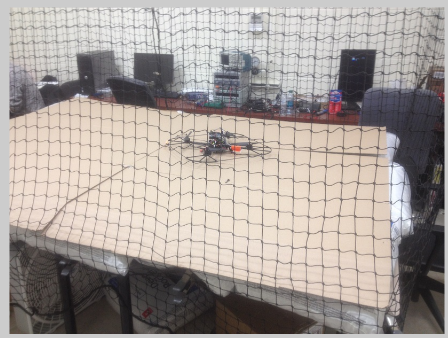

Fig. 3. Experimental test bed

where T is the time constant, h is the sampling time ,u is the filter input , y is the filter output and t_k is the k^{th} time stamp. For the test we select $h = 0.001$ and $T = 0.09$.

We carried out three different tests on the quadrotor in a 1m $\times$ 3 m $\times$ 2.5 m high netted test area, as shown in the Fig. 3. All the system parameters and controller parameters were recorded by a remote data acquisition and storage system via the on-board ZigBee communication module with a sampling rate of 1 ms. The following controller parameters were used: $M = 1.2$, I =dig$\{.005, .005, .008\}$ $k_p = 35, k_d = 6, k_1 = 3, \tau = 10$. The standard Hummingbird UAV is not designed for inverted flight, so experiments for large angle maneuvers are pending modification of the platform. Below we report the response of the geometric UDE controller to disturbances when flying in the upright equilibrium configuration.

A. Test 1

For this test we tested the controller performances on the quad rotor without external disturbance. We assumed that the parametric uncertainty and modeling errors were non-zero. Reference inputs were given via remote control module and data were recorded over 17s. Results are presented in Fig. 4 and Fig. 5. According to the Fig. 4, scalar error $\mathscr{E}$ lies with

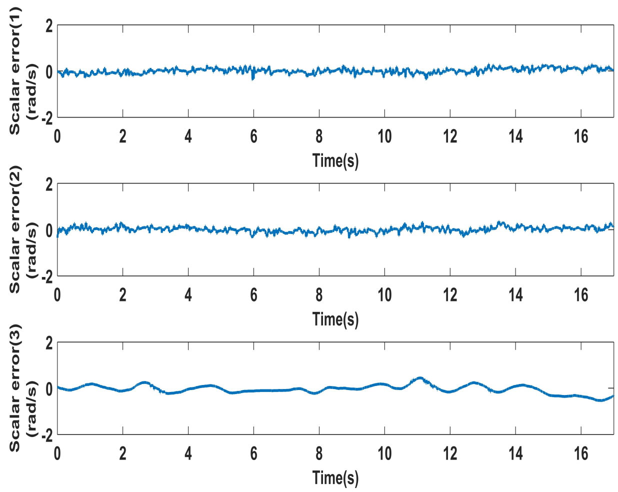

Fig. 4. Plot of $\mathscr{E}$(Scalar error) under parametric uncertainty without external disturbance and with reference input

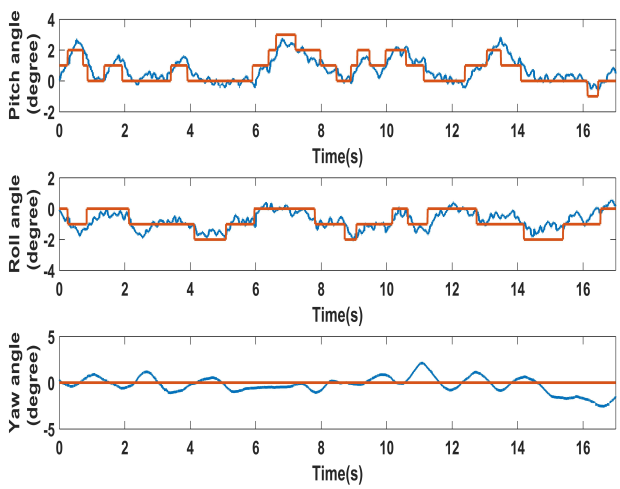

Fig. 5. Plot of angles and reference signal under parametric uncertainty without external disturbance,Red(reference signal),Blue(Actual angle)

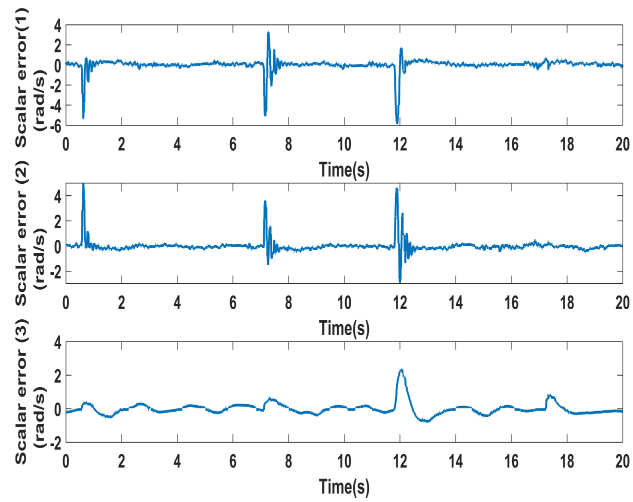

Fig. 6. Plot of $\mathscr{E}$(scalar error) under parametric uncertainty with external impulse disturbance and with reference input

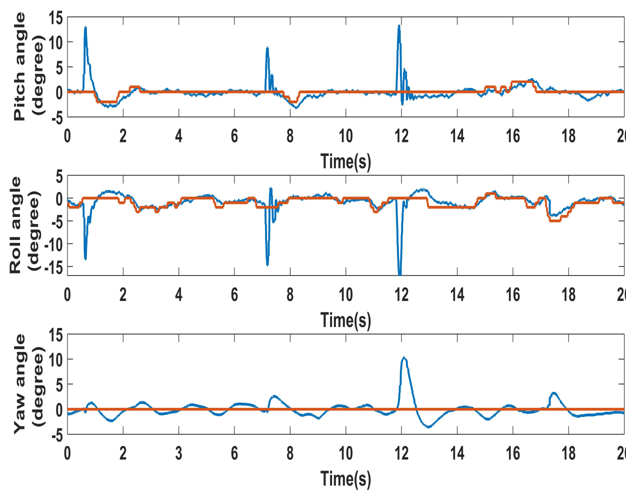

Fig. 7. Plot of angles and reference signal under parametric uncertainty and external impulse disturbance Red(reference signal),Blue(Actual angle)

in -0.2 rad/s and 0.2 rad/s range. Fig. 5 shows the system is tracking the reference input signal during the test.

B. *Test* 2

For this test we tested the controller performances on the quad rotor with external disturbance applied manually by hand in $+$pitch and $-$roll direction at 0.6 s , 7.18 s and 11.8 s . We assumed that the parametric uncertainty and modeling errors were non-zero. Reference inputs were given via remote control module and data were recorded over 20 s. Obtained results are presented in Fig. 6 and Fig. 7. Fig. 6 shows that after the first disturbance, the system took approximately .5 s to recover to within ± 0.1 rad/s of $\mathscr{E}$. Likewise, the time taken for $\mathscr{E}$ to recover to within ± 0.1 rad/s for the 2^{nd} and 3^{rd} cases is approximately 0.7 s and 0.5 s, respectively. Fig. 7 shows the system is tracking the reference input signal during the test.

C. *Test* 3

In this test we tested the closed-loop performance of the quadrotor with matched input disturbance $[13\sin(3t), 12\sin(2t), 2\sin(5t)]$ added in software. Reference inputs were given via remote control module and data were recorded over 20 s. Results are presented in Figs. 8–9.

VI. Conclusion

We have implemented an intrinsic geometric UDE controller on $SO(3)$, to control rigid-body attitude in the presence of disturbances and modeling error. The proposed control system was tested in simulation and on an actual quad rotor system. Simulation results suggest the ability to handle large maneuvers. The experimental platform is being

Margin requirements for the other pages
Paper size this page US Letter

54 pt
0.75 in
19.1 mm

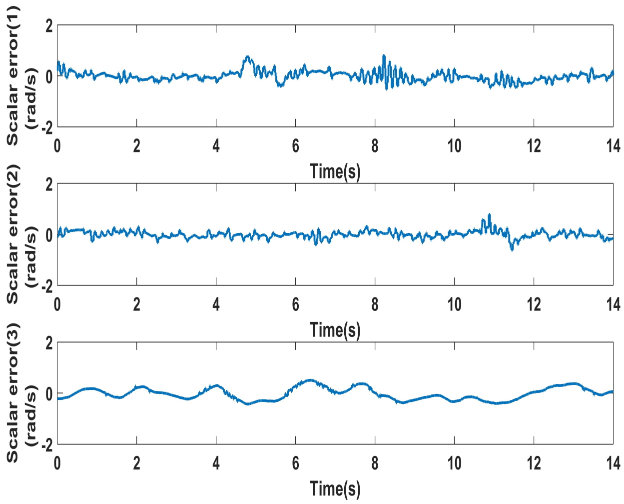

Fig. 8. Plot of $\mathscr{E}$ (scalar error) under parametric uncertainty and sinusoidal disturbance and with reference input

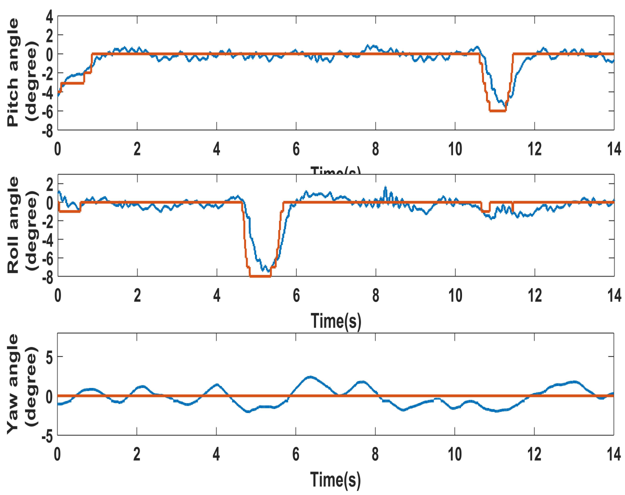

Fig. 9. Angles and reference signal under parametric uncertainty and sinusoidal disturbance. Red curve is the reference signal, blue curve is the actual angle.

modified to allow testing of large roll or pitch maneuvers. Preliminary experimental results for small initial error, time-varying disturbances, and parameter uncertainty are promising.

ACKNOWLEDGMENT

The authors wish to thank Mr Lu Qi for help with the quadrotor experiments.

REFERENCES

[1] Q.-C. Zhong and D. Rees. "Control of uncertain LTI systems based on an uncertainty and disturbance estimator. " *Journal of Dyn. Sys. Meas. Con.Trans. ASME*, Vol. 126, No. 4, 2004, pp. 905–910.
[2] S. Talole and S. Phadke. "Robust input-output linearisation using uncertainty and disturbance estimation." *Int. J. Control*, Vol. 82, No. 10, 2009, pp. 1794–1803.
[3] B. Ren and Q.-C. Zhong. " UDE-based robust control of variable-speed wind turbines. " *In Proc.The 39th Annual Conference of the IEEE Industrial Electronics Society (IECON2013)*, Vienna, Austria, 2013
[4] S. Talole, T. S. Chandar, and J. P. Kolhe. "Design and experimental validation of UDE based controller observer structure for robust input-output linearisation." *Int. J. Control*, Vol. 84, No. 5, 2011, pp. 969–984.
[5] R. K. Stobart and Q.C. Zhong. " Uncertainty and disturbance estimator (UDE)-based control for uncertain LTISISO systems with state delays." *Journal of Dyn. Sys.Meas. Con.Trans. ASME*, Vol. 133, No. 2, 2011, pp. 1–6.
[6] A. Kuperman and Q.-C. Zhong. " Robust control of uncertain nonlinear systems with state delays based on an uncertainty and disturbance estimator." *International Journal of Robust and Nonlinear Control*, Vol. 21, No. 1, Mar. 2010 , pp. 79–92.
[7] Beibei Ren and Qing-Chang Zhong, " UDE-Based Robust Control for a Class of Non-Affine Nonlinear Systems. " *Proceedings of the ASME 2013 Dynamic Systems and Control Conference*, Vol(3),Oct 2013, pp. V003T34A004, doi:10.1115/DSCC2013-3807
[8] A. D. Lewis "Is it worth learning differential geometric methods for modelling and control of mechanical systems," *Robotica*, Vol. 25, No. 6, Nov. 2007, pp. 765–777.
[9] T. Lee, "Robust adaptive tracking on SO(3) with an application to the attitude dynamics of a quadrotor UAV," *IEEE Transactions on Control Systems Technology*, vol. 21, no. 5, 2013, pp.1924–1930. doi:10.1109/TCST.2012.2209887.
[10] A. Bloch, *Nonholonomic Mechanics and Control*, Interdisciplinary Applied Mathematics. Springer-Verlag, 2003, vol. 24.
[11] F. Bullo and A. Lewis, *Geometric Control of Mechanical Systems*. Texts in Applied Mathematics. New York: Springer-Verlag, 2005,
[12] F. Bullo and R. M. Murray, "Tracking for fully actuated mechanical systems: a geometric framework," Automatica, vol. 35, no. 1, pp. 17–34, 1999.
[13] D. H. S. Maithripala, J. Berg, and W. P. Dayawansa, "Almost-Global Tracking of Simple Mechanical Systems on a General Class of Lie Groups," IEEE Transactions on Automatic Control, vol. 51, no. 2, pp. 216–225, 2006.
[14] D. H. S. Maithripala, W. P. Dayawansa, and J. M. Berg, "Intrinsic observer-based stabilization for simple mechanical systems on Lie groups," SIAM J. Control Optim., vol. 44, no. 5, pp. 1691–1711, Oct. 2005.
[15] T. Lee, M. Leok, and N. McClamroch, "Geometric tracking control of a quadrotor UAV on SE(3)," Proceedings of the IEEE Conference on Decision and Control, 2010, pp. 5420–5425.
[16] D. H. S. Maithripala and J. M. Berg, "Geometric pid control for almost-global stabilization of a quadrotor with parameter error and constant disturbances," Proceedings of the ASME Dynamic Systems and Control Conference, San Antonio, USA, October 22–24 2014.
[17] D. E. Koditschek, "The application of total energy as a lyapunov function for mechanical control systems," Contemporary Mathematics, vol. 97, pp. 131–157, February 1989.
[18] T. Frankel, *The Geometry of Physics: An Introduction*. Cambridge University Press, 1997.

54 pt
0.75 in
19.1 mm

54 pt
0.75 in
19.1 mm

54 pt
0.75 in
19.1 mm